CDF note 11035
Version 2.5

Measurement of the Leptonic Forward-Backward Asymmetry of $t\bar{t}$ Production and Decay in the Dilepton Final State and Combination of Charge Weighted Leptonic $A_{\mathbf{FB}}$ at CDF

The CDF Collaboration
URL http://www-cdf.fnal.gov
(Dated: June 3, 2014)

We have measured the charge weighted leptonic forward-backward asymmetry of $t\bar{t}$ events in the dilepton final state using 9.1 fb^{-1} of data, corresponding to the full CDF dataset. The inclusive $A_{\rm FB}^{\rm lep}$ is measured to be $A_{\rm FB}^{\rm lep} = 0.072 \pm 0.052(\text{stat.}) \pm 0.030(\text{sys.}) = 0.072 \pm 0.060$. This result is consistent with the NLO standard model expectation of $A_{\rm FB}^{\rm lep} = 0.038 \pm 0.003$. However, it is also consistent with the CDF measurement in the lepton + jets channel of $A_{\rm FB}^{\rm lep} = 0.094 \pm 0.024^{+0.022}_{-0.017}$, which is almost 2σ away from the NLO SM prediction. We also combined the $A_{\rm FB}^{\rm lep}$ measurement in the dilepton final state with the same measurement in the lepton+jets final state, and provided the best measurement of the $A_{\rm FB}^{\rm lep}$ at CDF. The combined result is $A_{\rm FB}^{\rm lep} = 0.090^{+0.028}_{-0.026}$, which is 2σ higher than the NLO SM prediction. In addition, we measured the forward-backward asymmetry of the η difference between the two leptons in each event. The result is $A_{\rm FB}^{\Delta\eta} = 0.076 \pm 0.072(\text{stat.}) \pm 0.039(\text{sys.}) = 0.076 \pm 0.082$, compared with NLO SM prediction of $A_{\rm FB}^{\Delta\eta} = 0.048 \pm 0.004$.

1. INTRODUCTION

1.1. Motivating the Leptonic $A_{\rm FB}$ Measurements

The Fermi National Accelerator Laboratory's Tevatron Run II collided protons against antiprotons at $\sqrt{s} = 1.96$ TeV from 2003 to 2011. Top and anti-top quark pairs ($t\bar{t}$) can be produced via quark-antiquark annihilation (85%) and gluon-gluon fusion (15%). The forward-backward asymmetry ($A_{\rm FB}$) of the $t\bar{t}$ system is an interesting observable, providing a chance to test the Standard Model (SM) and to probe physics beyond the SM. At leading order the SM predicts the differential cross section to be symmetric in polar angle θ if the beam line is chosen as the zenith direction, implying no $A_{\rm FB}$. However, at NLO the SM predicts a slight $A_{\rm FB}$ in the $t\bar{t}$ system at 0.088±0.006 [1]. If particles beyond the SM are considered, the $A_{\rm FB}$ can be drastically changed (higher or lower) because of interference among diagrams [2, 3].

Previous measurements of $A_{\rm FB}$ from $t\bar{t}$ events with CDF using 9.4 fb^{-1} and D0 using 5.4 fb^{-1} data in the lepton+jets signature have indicated a larger forward-backward asymmetry ($A_{\rm FB}$) [4, 5] than would be expected from the SM. A similar measurement was done at CDF with the dilepton final state with 5.1 fb^{-1} data [6] which also shows a larger $A_{\rm FB}$ than expected. The asymmetry in the differential cross section of the $t\bar{t}$ system can also be probed in other ways. For example, the angular distribution of cross section of $t\bar{t}$ system has been studied in the lepton + jets final state at CDF [7], observing that the excess is mostly in the coefficient of the linear dependent term of cosθ in the $t\bar{t}$ differential cross section.

While the $A_{\rm FB}$ of the $t\bar{t}$ system is a valuable observable, an alternative observable, which is also interesting and important, is the forward-backward asymmetry of the decayed leptons of the $t\bar{t}$ system, the so called leptonic $A_{\rm FB}$. In the scenario where t→Wb and the W decays leptonically, the asymmetric production of the $t\bar{t}$ system also results in an asymmetric distribution of the decayed leptons. In addition, if the $t\bar{t}$ pair is produced via resonance production and decay of hypothesized polarized particles beyond the SM (like the two polarized axigluon models listed in Table I), the polarization of the $t\bar{t}$ system carried over from its parent particle also affects the direction of its daughter leptons, even though the $A_{\rm FB}$ of the $t\bar{t}$ system itself isn't affected by the polarization [8].

There are also experimental advantages in measuring the leptonic $A_{\rm FB}$ relative to the full $A_{\rm FB}$ of the $t\bar{t}$ system itself. The ability to reconstruct the 4-momentum of both the top and anti-top is imperfect, and can have large systematic uncertainties. Furthermore, the reconstruction of the $t\bar{t}$ system is especially difficult in the dilepton final state, due to the ambiguity of the b-jet and the $\bar{b}$-jet, and the distribution of the $\not\!\!E_T$ between the two neutrinos. On the other hand, the measurement of the leptonic $A_{\rm FB}$ mainly relies on the directions of the lepton paths in the detector, which are measured with high precision. Thus, the measurement of leptonic $A_{\rm FB}$ has the potential to be done with better precision and less systematic uncertainty, and could yield information about both the produced $A_{\rm FB}$ from the $t\bar{t}$ system as well as its polarization.

In this note we first report the measurement of leptonic $A_{\rm FB}$ in the dilepton final state, then show the best estimate of the charge weighted leptonic $A_{\rm FB}$ at CDF by combining the measurement in the dilepton final state with the same measurement in the lepton+jets final state.

1.2. Defining the Leptonic $A_{\rm FB}$ and Expectations from Various Models

The leptonic $A_{\rm FB}$ of the $t\bar{t}$ system can be defined in two ways in the dilepton final state that have been found to be useful: the charge weighted $A_{\rm FB}$ of single leptons, and the $A_{\rm FB}$ in the relative direction between the two leptons. In the scenario of CP conservation, we can combine the $A_{\rm FB}$ of positive and negative leptons together and define the charge weighted leptonic $A_{\rm FB}$ as

$$A_{\rm FB}^{\rm lep} = \frac{N(q\eta_l > 0) - N(q\eta_l < 0)}{N(q\eta_l > 0) + N(q\eta_l < 0)} \tag{1}$$

where N is the number of leptons, q is the lepton charge, and η is the pseudorapidity of the lepton. Similarly, since there are two leptons detected in each event in dilepton final state, the leptonic $A_{\rm FB}$ in the relative directions between the two opposite charged leptons of an event can be defined as

$$A_{\rm FB}^{\Delta\eta} = \frac{N(\Delta\eta > 0) - N(\Delta\eta < 0)}{N(\Delta\eta > 0) + N(\Delta\eta < 0)} \tag{2}$$

where $\Delta\eta = \eta_{l^+} - \eta_{l^-}$.

Due to the low branching fraction of dilepton final state, both results are expected to be statistically limited. We will provide the measurement of charge weighted leptonic $A_{\rm FB}$ ($A_{\rm FB}^{\rm lep}$) as our major measurement since the statistical

Model	$A_{\rm FB}^{\rm lep}$ (Generator Level)	$A_{\rm FB}^{\Delta\eta}$ (Generator Level)	Description
AxiL	-0.063(2)	-0.092(3)	Tree-level left-handed axigluon (m = 200 GeV/c^2, Γ = 50 GeV/c^2)
AxiR	0.151(2)	0.218(3)	Tree-level right-handed axigluon (m = 200 GeV/c^2, Γ = 50 GeV/c^2)
Axi0	0.050(2)	0.066(3)	Tree-level unpolarized axigluon (m = 200 GeV/c^2, Γ = 50 GeV/c^2)
ALPGEN	0.003(1)	0.003(2)	Tree-level Standard Model
PYTHIA	0.000(1)	0.001(1)	LO Standard Model
POWHEG	0.024(1)	0.030(1)	NLO Standard Model
Theory	0.038(3)	0.048(4)	NLO SM calculation

TABLE I. The MC samples used to study the $t\bar{t}$ system in this analysis, together with the generator level $A_{\rm FB}^{\rm lep}$ and $A_{\rm FB}^{\Delta\eta}$ predicted by the corresponding physics model, as well as the NLO SM calculation [1]. The uncertainties listed with the MC samples are statistical only. We note that unless specified otherwise, the POWHEG $t\bar{t}$ sample is used as our default $t\bar{t}$ sample.

uncertainty is smaller in such a scenario as we have two lepton measurements from each event and the leptons are largely uncorrelated. We will also show the measurement of $A_{\rm FB}^{\Delta\eta}$ even though it provides a less sensitive measurement, but is expected to have a larger absolute value.

Since many models of new physics predict very different values of $A_{\rm FB}^{\rm lep}$, we looked at a variety of MC samples. This will also assist with the validation of the methodology we use to extrapolate from $A_{\rm FB}$ observed to parton level $A_{\rm FB}$. We used three SM MC samples generated with PYTHIA [9], ALPGEN [10] and POWHEG [11] and three MC samples with particles beyond the SM [8] generated with MADGRAPH [12] as our reference models. They are:

- PYTHIA: Leading order SM, generated and showered by PYTHIA.
- ALPGEN: Tree-level SM, generated by ALPGEN and showered by PYTHIA.
- POWHEG: Next-to-leading-order SM, with QCD correction, but without EWK correction, generated by POWHEG and showered by PYTHIA. Note that the EWK correction of $A_{\rm FB}$ is about 26%.
- AxiL: Tree-level left-handed axigluon (m = 200 GeV/c^2, Γ = 50 GeV/c^2), generated by MADGRAPH and showered by PYTHIA.
- AxiR: Tree-level right-handed axigluon (m = 200 GeV/c^2, Γ = 50 GeV/c^2), generated by MADGRAPH and showered by PYTHIA.
- Axi0: Tree-level unpolarized axigluon (m = 200 GeV/c^2, Γ = 50 GeV/c^2), generated by MADGRAPH and showered by PYTHIA.

Table I shows the values of $A_{\rm FB}^{\rm lep}$ and $A_{\rm FB}^{\Delta\eta}$ at generator level for each MC sample, together with the NLO theoretical calculation with QCD and EWK correction from Ref. [1]. Note that the three MC samples with axigluons have the same inclusive $A_{\rm FB}$ values of the $t\bar{t}$ system (∼12%), while the different polarizations result in different values of the leptonic $A_{\rm FB}$.

The measurement of the $A_{\rm FB}^{\rm lep}$ of the $t\bar{t}$ system has been performed in the lepton+jets final state at CDF with the full dataset [13], and a $\sim 2\sigma$ deviation from NLO SM prediction is observed. There are similar measurements from D0 with both lepton+jets and dilepton final states [14, 15], which show results that are consistent with the NLO SM prediction.

This note summarizes the results of the analysis studying the leptonic $A_{\rm FB}$ of $t\bar{t}$ system in the dilepton final state with essentially the same standard event selection criteria as used in the $t\bar{t}$ cross section measurement [16].

2. EVENT SELECTION AND BACKGROUND ESTIMATION

In this analysis, we used the data collected by the CDF detector during Run II corresponding to an integrated luminosity of 9.1 fb^{-1}. We followed the event selection criteria that was used in measuring the top pair cross section in the dilepton final state [16], with the dilepton invariant mass requirement raised to 10 GeV/c^2 to prevent potential mismodelling in low dilepton invariant mass region. The event selection criteria is summarized in Table II.

Baseline Cuts	Exactly two leptons with $E_{\rm T} > 20$ GeV and passing standard identification requirements -At least one trigger lepton -At least one tight and isolated lepton -At most one lepton can be loose and/or non-isolated
	$\not\!\!E_T > 25$ GeV, but $\not\!\!E_T > 50$ GeV when there is any lepton or jet within 20° of the direction of $\not\!\!E_T$
	MetSig $(= \frac{\not\!\!E_T}{\sqrt{E_T^{sum}}}) > 4\ \sqrt{\rm GeV}$ for ee and $\mu\mu$ events where 76 GeV/c^2 < m_{ll} < 106 GeV/c^2
	$m_{ll} > 10$ GeV/c^2
Signal Cuts	Two or more jets with $E_{\rm T} > 15$ GeV within $\|\eta\| < 2.5$
	$H_{\rm T} > 200$ GeV
	Opposite sign of two leptons

TABLE II. The event selection requirements to select $t\bar{t}$ events in the dilepton final state. We note that the m_{ll} cut raised from 5 GeV/c^2 to 10 GeV/c^2 from the cross section measurement with the same final state at CDF [16] .

Several physical processes can mimic the signature of top pairs in the dilepton final state, such as DY+jets, W+jets, diboson production (WW, WZ, ZZ and Wγ), and situations where one of the W bosons from $t\bar{t}$ decays hadronically and one jet is misidentified as a lepton. We followed the same background estimation techniques as used in the top pair cross section measurement, but with minor improvements. The prescription is a mixture of Monte Carlo simulations and data-based techniques. A collection of MC samples are generated for this purpose. The WW, WZ and ZZ processes are simulated with PYTHIA MC generator [9], the Wγ process is simulated with the BAUR MC generator [17], and the DY+jets processes are simulated with the ALPGEN MC generator [10]. PYTHIA is used for modelling parton showering and underlying events for all background MC simulations. A GEANT-based simulation, CDFSIM [18, 19], is used to model the CDF detector, including luminosity weighted profiles of the extra collisions in the event. Using the same method as the standard dilepton cross section, the background rate from the diboson processes are obtained by normalizing the corresponding MC samples to the integrated luminosity collected in data with their predicted production cross section, and correcting for trigger and detector based inefficiencies that are not well modelled in the simulation. The contamination from the W+jets process is estimated using the standard data-based technique where the probability of a jet faking a lepton is derived from a separate dataset [16].

The contamination from DY+jets where Z/γ^* decays to two electrons or two muons are done with a data-MC hybrid method. The MC samples are normalized to data after subtracting off components other than Z/$\gamma^* \to$ ee/$\mu\mu$ according to the number of events within the window of 76 GeV/c^2 < m_{ll} < 106 GeV/c^2 after requiring high $\not\!\!E_T$. As an improvement from the cross section measurement [16], the contamination from DY $\to \tau\tau$ and DY $\to$ ee + $\mu\mu$ which are misidentified as eμ final state is estimated using a more sophisticated method which applies two scale factors derived with the DY $\to$ ee + $\mu\mu$ process within the window of 76 GeV/c^2 < m_{ll} < 106 GeV/c^2 and corrects for the mismodeling of the total event rate and $\not\!\!E_T$ distribution in MC simulations.

A new category of background event is to separate out $t\bar{t}$ events where one of the W's from the top pair decays hadronically, and one jet in the event is misidentified as a lepton. This constitutes a non-negligible portion of the events in our sample. Since at least one of the leptons identified in such events are not from W leptonic decay, the lepton η's don't follow the same distribution as $t\bar{t}$ dilepton signal. We estimate this contribution with the POWHEG $t\bar{t}$ MC sample after normalizing the sample with the cross section to the best theoretical prediction of 7.4 pb [20], and put these events into a background category, labelled "$t\bar{t}$ Non-Dilepton".

Table III shows the expected number of background processes and $t\bar{t}$ signal estimated with POWHEG $t\bar{t}$ MC sample, together with the observed number of events in signal region, listed by lepton flavor. As a check we consider the comparison of the background modelling with various kinematic variables for our final state. Fig. 1 shows the estimated distribution of lepton p_T and $\not\!\!E_T$ from background components along with $t\bar{t}$ and overlaid with data. The estimations agree well with the observed distributions.

3. METHODOLOGY FOR MEASURING $A_{\rm FB}$

With our dataset in hand and our backgrounds well understood, we are now ready to measure the leptonic $A_{\rm FB}$ for $t\bar{t}$ events. As defined in Eqn (1), the charge weighted leptonic $A_{\rm FB}$ is the number of forward leptons minus the number of backward leptons divided by the sum. Due to the limited detector coverage ($|\eta|$ <1.1 for central electrons and

CDF Run II Preliminary (9.1 fb^{-1})

$t\bar{t}$ Dilepton Signal Events per Dilepton Flavor Category				
Source	ee	$\mu\mu$	eμ	$\ell\ell$
WW	5.5±1.1	4.2±0.8	11.4±2.3	21.1±4.2
WZ	2.7±0.5	1.6±0.3	1.6±0.3	5.8±1.0
ZZ	1.7±0.3	1.3±0.2	0.7±0.1	3.7±0.5
Wγ	0.7±0.8	-	-	0.7±0.8
DY$\rightarrow \tau\tau$	4.4±0.8	3.4±0.6	9.3±1.6	17.0±2.8
DY$\rightarrow ee + \mu\mu$	19.8±2.1	10.4±1.8	3.3±1.5	33.5±3.9
W+jets Fakes	12.4±3.8	14.6±4.7	36.8±11.3	63.8±17.0
$t\bar{t}$ Non-Dilepton	3.3±0.2	3.3±0.2	8.0±0.4	14.6±0.8
Total background	50.5±5.8	38.8±5.6	71.0±12.7	160.3±21.2
$t\bar{t}$ ($\sigma = 7.4$ pb)	96.0±4.6	90.8±4.4	221.4±10.6	408.2±19.4
Total SM expectation	146.4±10.2	129.6±9.7	292.4±23.1	568.5±40.3
Observed	147	139	283	569

TABLE III. Table of the expected number of events in data corresponding to 9.1fb^{-1} with the observed number of events passing all event selections, listed by lepton flavors.

muons and $|\eta|$ <2 for forward electrons), the imperfect detector acceptance, the smearing due to detector response and contamination from non-$t\bar{t}$ sources, corrections and an extrapolation procedure is needed to measure the parton level leptonic $A_{\rm FB}$ from data. To do so, we follow the same procedure used in measuring the charge weighted leptonic $t\bar{t}$ $A_{\rm FB}$ in the lepton+jets final state [13]. In this section, we validate this methodology for the dilepton final state, as well as some custom modification made to apply this methodology to this channel. Note that while we will be using the same methodology for both $A_{\rm FB}^{\rm lep}$ and $A_{\rm FB}^{\Delta\eta}$, our description here will describe $A_{\rm FB}^{\rm lep}$ explicitly first, and then give the results of the validation procedure for $A_{\rm FB}^{\Delta\eta}$.

3.1. Methodology Overview

Fig 2 shows the $q\eta_l$ distribution at generator level for the six $t\bar{t}$ MC samples described in Table I before any selection requirements. We note that they span the range of possible values of $A_{\rm FB}^{\rm lep}$ from -6% to 15%. The $q\eta_l$ distribution of leptons can be decomposed into a symmetric part and an asymmetric part using the following formulas:

$$S(|q\eta_l|) = \frac{N(|q\eta_l|) + N(-|q\eta_l|)}{2} \tag{3a}$$

$$A(|q\eta_l|) = \frac{N(|q\eta_l|) - N(-|q\eta_l|)}{N(|q\eta_l|) + N(-|q\eta_l|)}. \tag{3b}$$

With this, the $A_{\rm FB}^{\rm lep}$ defined in Eqn. 1 can be rewritten in terms of S($|q\eta_l|$) and A($|q\eta_l|$) as:

$$A_{\rm FB}^{\rm lep} = \frac{N(q\eta_l > 0) - N(q\eta_l < 0)}{N(q\eta_l > 0) + N(q\eta_l < 0)} \tag{4a}$$

$$= \frac{\int_0^\infty {\rm d}(|q\eta_l|)\ [A(|q\eta_l|) \cdot S(|q\eta_l|)]}{\int_0^\infty {\rm d}(|q\eta_l|)\ S(|q\eta_l|)} \tag{4b}$$

With this description, the measurement methodology can be simplified by the following three assumptions which we will validate:

- The symmetric part of $q\eta_l$ distributions at generator level are so similar among all models that choosing only one for our measurement introduces an uncertainty that is tiny compared to our dominant uncertainties.
- The asymmetric part of $q\eta_l$ distribution for the various models can be described with a functional form of

$$A(|q\eta_l|) = a \cdot \tanh[\frac{1}{2} \cdot |q\eta_l|] \tag{5}$$

  where a is a free parameter that is directly related to the final asymmetry.

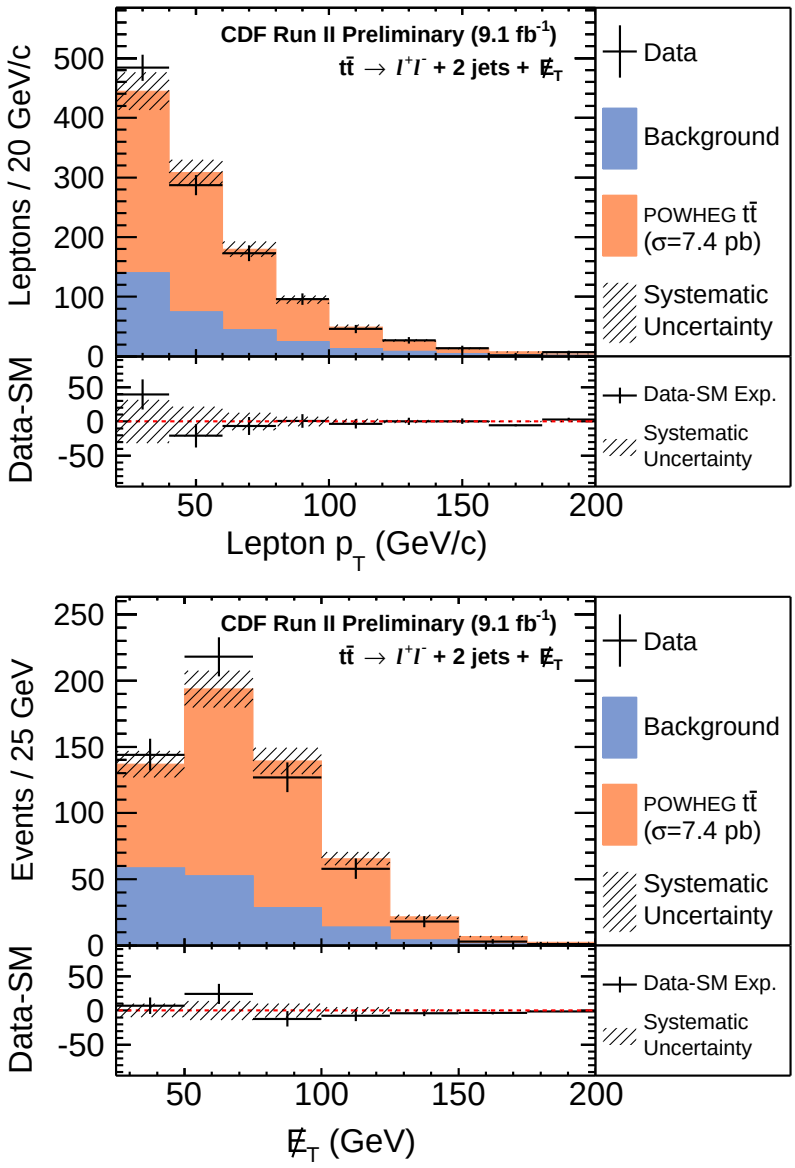

FIG. 1. A comparison of the observed and predicted values of the lepton p_T and $\not\!\!E_T$ in the signal region for the dilepton final state. The data is consistent with expectations within uncertainties.

- With a reasonable binning choice of $q\eta_l$ distribution, the bin-to-bin migration of events due to detector smearing is small, and has no measurable effect on the final value of $A_{\rm FB}^{\rm lep}$.

The strategy of this method is to measure the free parameter a from data, and use the symmetric part of the generator level $q\eta_l$ distribution from $t\bar{t}$ MC to get the parton level $A_{\rm FB}^{\rm lep}$. Note that this methodology naturally corrects for the detector response and limited detector η coverage at the same time.

In the subsequent subsections, we will show how well this methodology works in the dilepton final state, first at the generator level where we can use high statistics, and then at the reconstructed level.

3.2. Methodology Validation at Generator Level

To test the assumptions that the small variations in the symmetric part of the $q\eta_l$ distribution at the generator level from different physical model don't affect the measurement, and that the asymmetric part can be effectively

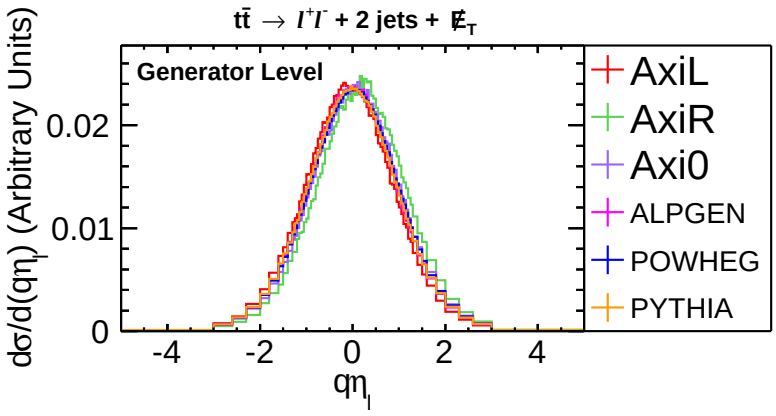

FIG. 2. The $q\eta_l$ distribution for leptons from MC samples with various physics models at generator level, before any selection requirements.

modelled by hyperbolic tangent function, we show that the methodology works at generator level to a high degree of precision, and only contributes a variation that is small compared to our final sensitivity.

Fig. 3 shows the symmetric part of $q\eta_l$ distribution from various $t\bar{t}$ MC samples, with two leptons per event. All samples show basic agreement with each other. For concreteness, in the final measurement we use the distribution from POWHEG $t\bar{t}$ MC, since that's the sample we have with largest statistics and is our best approximation to the SM. We assign the difference obtained using different MC samples as our systematic uncertainty for the symmetric modelling and note for now that it is small compared to the final uncertainty.

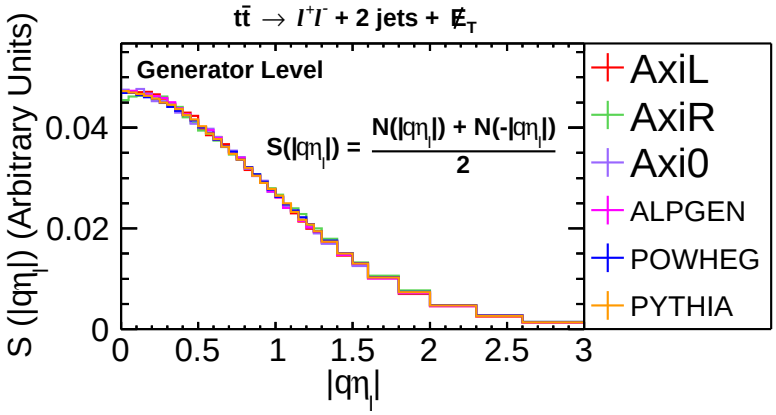

FIG. 3. The symmetric part of the $q\eta_l$ distribution for both positive and negative leptons from MC samples at generator level with various physics models.

Fig. 4 shows the asymmetric part of the $q\eta_l$ distribution together with fit of Eqn. 5. For the different models, the hyperbolic tangent function describes the asymmetric part reasonably well for $|q\eta_l| < 2.5$. After $|q\eta_l| = 2.5$, the asymmetric parts from some of the MC samples show some deviation from the fit functions. While this could, in principle, be a problem, we note that according to Eqn. 4b, the inclusive $A_{\rm FB}^{\rm lep}$ is the asymmetric part weighted by the symmetric part. As shown by Fig. 3, the symmetric part drops quickly as a function of $q\eta_l$, thus the contribution to $A_{\rm FB}^{\rm lep}$ from region above $|q\eta_l| = 2.5$ is small. To show this quantitatively, Fig. 5 shows the symmetric part times asymmetric part of $q\eta_l$ distribution as a function of $q\eta_l$, normalized by the integral of the symmetric part from the POWHEG $t\bar{t}$ sample. The integral gives the inclusive $A_{\rm FB}^{\rm lep}$ of this sample. We note that 89% of $A_{\rm FB}^{\rm lep}$ comes from region where $|q\eta_l| < 2.0$, which is the region with our detector coverage. A total of 96% of $A_{\rm FB}^{\rm lep}$ comes from region where $|q\eta_l| < 2.5$, where the tanh fit works well. So the effect of potential mismodelling of asymmetric part distribution is very small compared to our systematic uncertainty in principle, and in practice will be shown to be small compared

to the dominant systematic uncertainties (although it will be included for completeness).

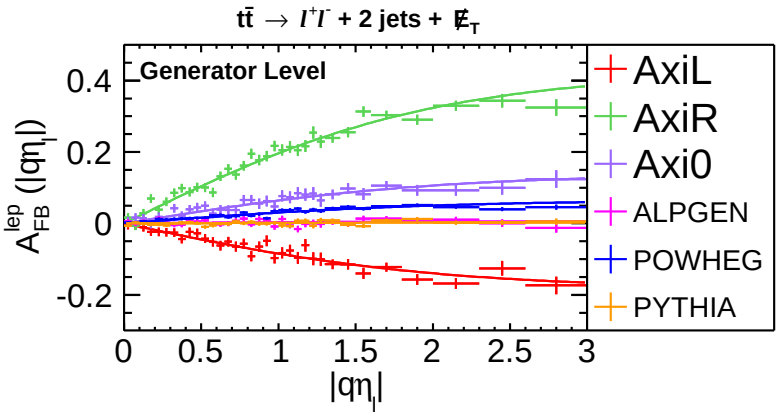

FIG. 4. The asymmetric part of the $q\eta_l$ distribution for both positive and negative leptons from MC samples at generator level with various physics models, with tanh fit.

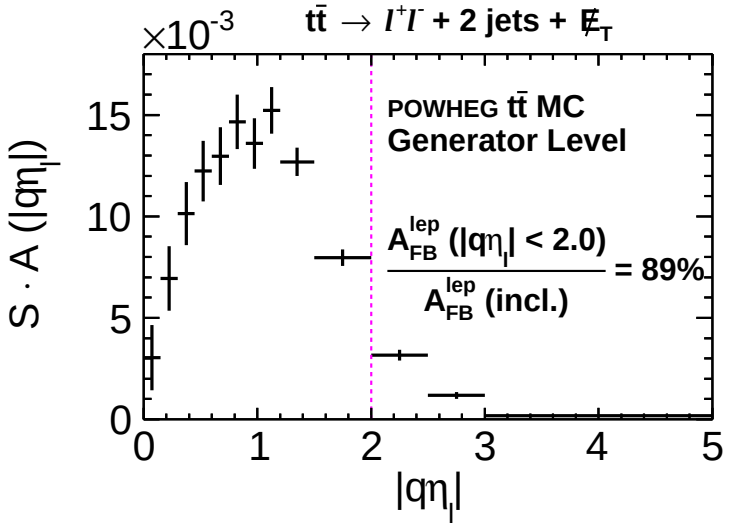

FIG. 5. The symmetric part times asymmetric part of $q\eta_l$ distribution as a function of $q\eta_l$, normalized by the integral of the symmetric part from POWHEG $t\bar{t}$ sample. The integral under the curve of this distribution gives the inclusive $A_{\rm FB}$ from POWHEG $t\bar{t}$ sample.

Fig 6 shows a comparison between the truth level $A_{\rm FB}^{\rm lep}$ from MC and the $A_{\rm FB}^{\rm lep}$ measured using our methodology for the six MC samples. There is no apparent bias in the measurement and the differences are at the 0.005 level, well below the dominant systematic uncertainty (which will be 0.03, and from background uncertainties). With our method well established at generator level, we move to the information after detector simulation and reconstruction.

3.3. Methodology Validation at Reconstructed Level

Since we have limited statistics, imperfect detector resolution and incomplete detector coverage, we next use simulated data from the different $t\bar{t}$ MC samples to see if there are any biases in our methodology or if further corrections are needed. The final methodology will be to use the fit of Eqn. 5 on the $q\eta_l$ distribution after detector simulation and

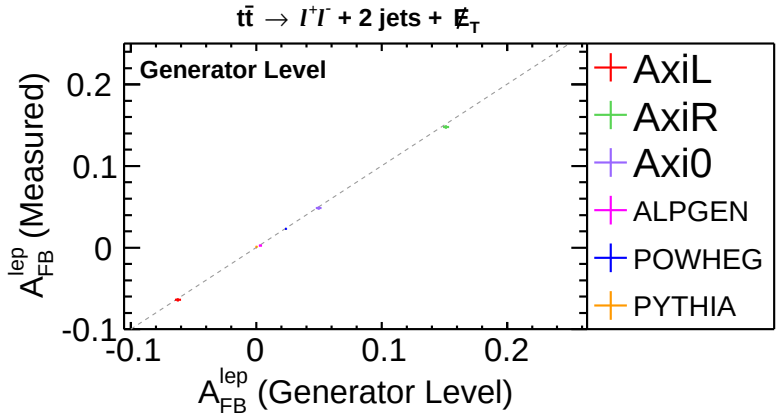

FIG. 6. A comparison between the truth level $A_{\rm FB}^{\rm lep}$ from MC and the $A_{\rm FB}^{\rm lep}$ as measured using our methodology with generator level information. The agreement is excellent. The dashed line indicates the location of the equal values, while the points (with very small error bars) are superimposed at their measured locations.

reconstruction from various $t\bar{t}$ MC samples, but using the generator results from POWHEG $t\bar{t}$ MC for the symmetric term. Our validation compares the measured $A_{\rm FB}^{\rm lep}$ to the $A_{\rm FB}^{\rm lep}$ in the corresponding MC sample at generator level.

Fig. 7 shows the reconstructed level asymmetric part of $q\eta_l$ from the $t\bar{t}$ MC samples together with the best fit of Eqn. 5. The results of the measured $A_{\rm FB}^{\rm lep}$ obtained are listed in Table IV together with the corresponding $A_{\rm FB}^{\rm lep}$ at generator level. Fig. 8 shows the comparison graphically. We note that with the method described above we get back to truth level $A_{\rm FB}^{\rm lep}$ within statistics with no noticeable bias. The differences are small compared to expected statistical uncertainty of around 0.05. To cover any potential bias caused by this method conservatively, we quote the difference between the measured parton level $A_{\rm FB}^{\rm lep}$ and the $A_{\rm FB}^{\rm lep}$ at generator level from POWHEG $t\bar{t}$ MC sample as the systematic uncertainty for asymmetric modelling.

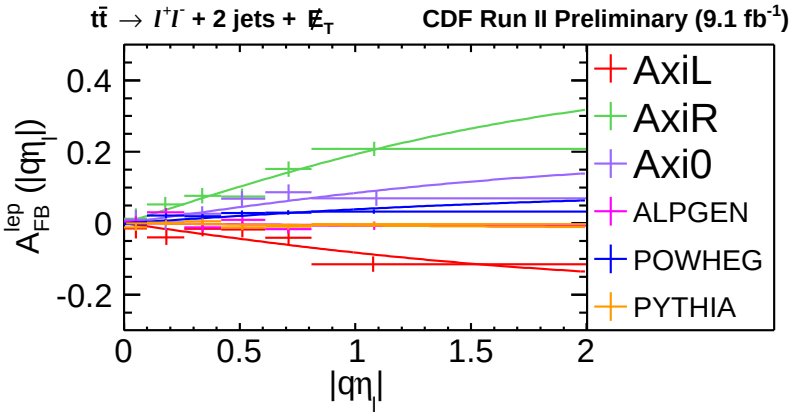

FIG. 7. The asymmetric part of the $q\eta_l$ distribution from the MC samples with various physics models after simulation, reconstruction and event selection.

Before moving to the final result, we quickly show that the same methodology works for measuring $A_{\rm FB}^{\Delta\eta}$. The results are shown in Fig. 9 and Table V.

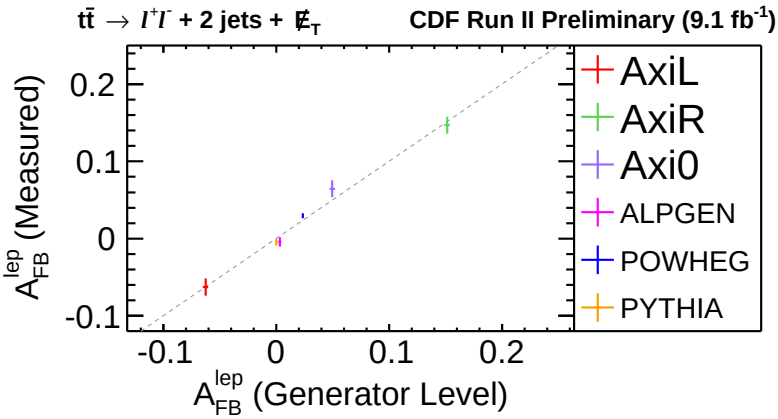

FIG. 8. The truth level $A_{\rm FB}^{\rm lep}$ from MC and the $A_{\rm FB}^{\rm lep}$ as measured using our methodology with reconstructed level information. No noticeable bias is observed. The dashed line indicates the location of equal values, while the points (with their corresponding error bars) are superimposed at their measured locations.

CDF Run II Preliminary (9.1 fb^{-1})

Model	$A_{\rm FB}^{\rm lep}$(Generator Level)	$A_{\rm FB}^{\rm lep}$(Measured)	Difference
AxiL	-0.063	-0.063±0.011	0.0001
AxiR	0.151	0.147±0.011	0.004
Axi0	0.050	0.065±0.011	-0.015
ALPGEN	0.003	-0.004±0.006	0.008
PYTHIA	0.000	-0.005±0.004	0.005
POWHEG	0.024	0.029±0.003	-0.006

Uncertainties are statistical only.

TABLE IV. A comparison of the generator level $A_{\rm FB}^{\rm lep}$ and our measured value after using the full analysis methodology on reconstructed $t\bar{t}$ events that have been through the full simulation and event selection procedure. Note that the difference is small compared to the final measurement uncertainty in the data which is around 0.05.

CDF Run II Preliminary (9.1 fb^{-1})

Model	$A_{\rm FB}^{\Delta\eta}$(Generator Level)	$A_{\rm FB}^{\Delta\eta}$(Measured)	Difference
AxiL	-0.092	-0.086±0.016	-0.006
AxiR	0.218	0.215±0.015	0.003
Axi0	0.066	0.092±0.015	-0.026
ALPGEN	0.003	-0.006±0.008	0.009
PYTHIA	0.001	-0.006±0.006	0.008
POWHEG	0.030	0.042±0.004	-0.012

Uncertainties are statistical only.

TABLE V. A comparison of the generator level $A_{\rm FB}^{\Delta\eta}$ and our measured value after using the full analysis methodology on reconstructed $t\bar{t}$ events that have been through the full simulation and event selection procedure. Note that the difference is small compared to the final measurement uncertainty in the data which is around 0.07.

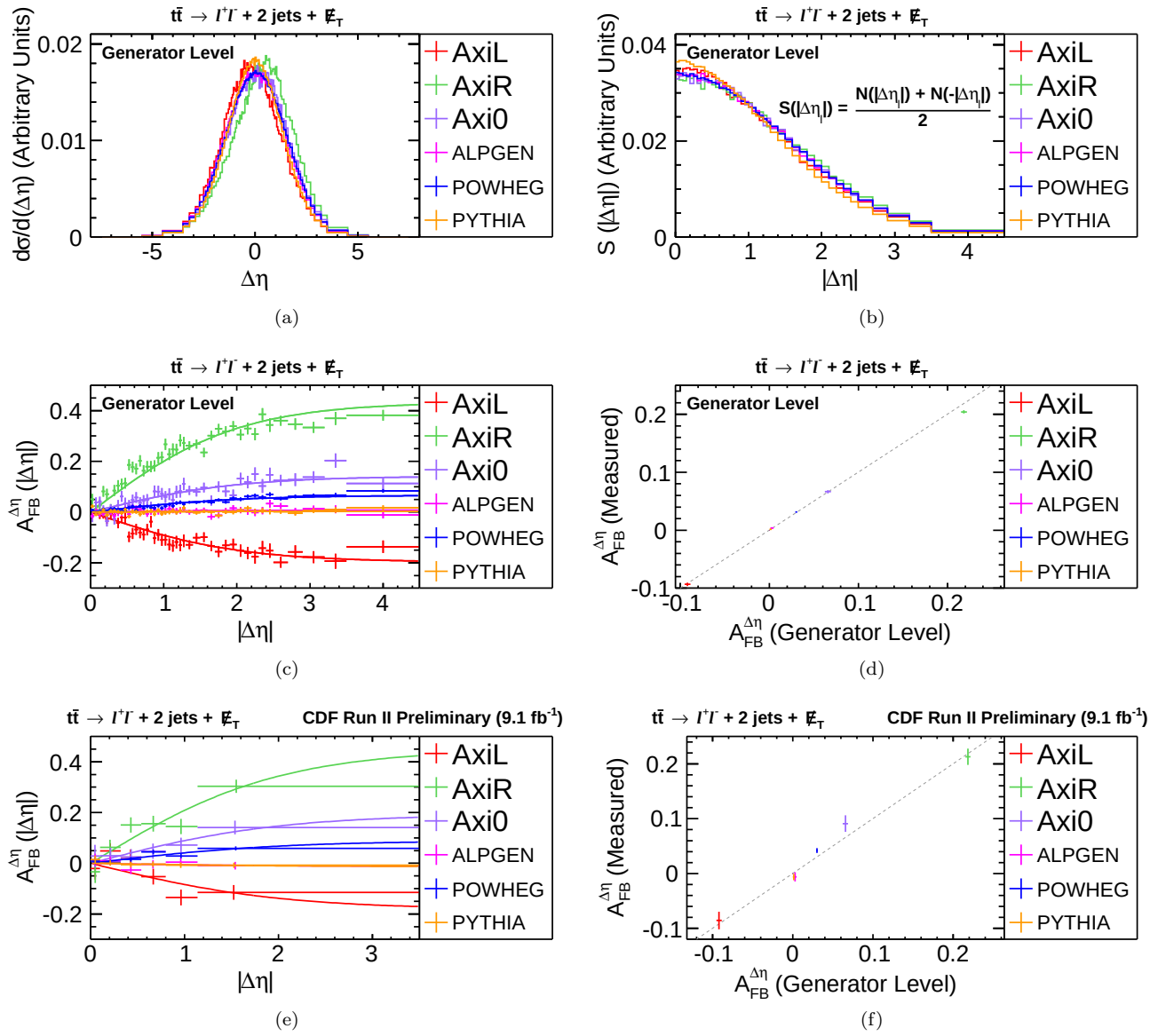

FIG. 9. The same results as in Figs. 2, 3, 4, 6, 7 and 8, but using $\Delta\eta$ instead of $q\eta_l$. These show that the same methodology will work for both measurements.

4. MEASURING $A_{\rm FB}$ FROM DATA

With the methodology validated for a variety of values of $A_{\rm FB}^{\rm lep}$ and $A_{\rm FB}^{\Delta\eta}$, we can take the data, subtract off the backgrounds and extrapolate to get the measured $A_{\rm FB}$. In this section, we first show the uncorrected $A_{\rm FB}$ obtained from data before and after subtracting off the background contamination (simply counting the number of events with $q\eta_l(\Delta\eta) > 0$ and $q\eta_l(\Delta\eta) < 0$), and then measure the parton level $A_{\rm FB}^{\rm lep}$ along with giving our estimate of the total uncertainties. The measurement of the $A_{\rm FB}^{\Delta\eta}$ follows that.

4.1. Measuring $A_{\rm FB}^{\rm lep}$ from the Data

With the signal region defined and background components estimated in Sec. 2, we are ready to look at the distribution of $q\eta_l$ and $\Delta\eta$ from data (before and after background subtraction) and compare to the SM expectations. The results are shown in Fig. 10 and Fig. 11 respectively. Table VI shows the expected individual uncorrected $A_{\rm FB}$ from simple counting for each background and from data, as well as our best estimation of the leptonic $A_{\rm FB}$ for the $t\bar{t}$ system observed in our detector by subtracting off the expected background contributions. The expected fractions of each background components and $t\bar{t}$ signal are also listed in this table.

CDF Run II Preliminary (9.1 fb^{-1})

Source	Uncorrected $A_{\rm FB}^{\rm lep}$	Uncorrected $A_{\rm FB}^{\Delta\eta}$	Fraction of SM expectation
WW	0.06±0.01	0.08±0.02	3.7%
WZ	-0.01±0.02	-0.01±0.03	1.0%
ZZ	-0.04±0.03	-0.08±0.04	0.6%
DY $\rightarrow$ ee + $\mu\mu$	-0.08±0.02	-0.18±0.03	5.9%
DY $\rightarrow \tau\tau$	-0.08±0.03	-0.13±0.04	3.0%
W+jets Fakes	-0.04±0.04	-0.06±0.05	11.2%
$t\bar{t}$ Non-Dilepton	-0.00±0.01	0.02±0.02	2.6%
Total Background	-0.04±0.02	-0.07±0.02	28.2%
POWHEG $t\bar{t}$	0.024±0.003	0.030±0.004	71.8%
Data	0.02±0.03	0.03±0.04	-
Background Subtracted Data	0.04±0.04	0.06±0.06	-

TABLE VI. The uncorrected $A_{\rm FB}^{\rm lep}$ and $A_{\rm FB}^{\Delta\eta}$ for backgrounds, POWHEG $t\bar{t}$ and data using a simple counting method. The expected fractions of each background and $t\bar{t}$ signal components are also listed. The uncertainties are statistical only.

Fig. 12 shows the symmetric part of $q\eta_l$ distribution from data after background subtraction along with the expectation from POWHEG $t\bar{t}$ MC. The data after background subtraction shows good agreement with expectations. Fig. 13 shows the best fit of Eqn. 5 on the asymmetric part of data after background subtraction. The $A_{\rm FB}^{\rm lep}$ retrieved from this fit is

$$A_{\rm FB}^{\rm lep} = 0.072 \pm 0.052(\text{stat.})$$

4.2. Systematic uncertainties for $A_{\rm FB}^{\rm lep}$

The systematic uncertainties are estimated using the same techniques as for the measurement of the leptonic $A_{\rm FB}$ of $t\bar{t}$ in the lepton+jets final state [13] with only small differences. As will be seen, the dominant uncertainty on the measurement is the statistical uncertainty, while the dominant systematic uncertainty is from the uncertainty on the rates and $q\eta_l$ distributions of the background components. The results are summarized in Table VII.

To estimate the effect on $A_{\rm FB}$ from both the normalization of the backgrounds and the shape variation, we generated two sets of pseudo-experiments. For the first set of pseudo-experiments, we estimated the uncertainty due to the fluctuation in the number and the shape of $t\bar{t}$ signal only. We used the POWHEG $t\bar{t}$ MC as our signal sample, and for each pseudo-experiment the number of $t\bar{t}$ events is normalized according to the expected $t\bar{t}$ event count with its total uncertainty (statistical and systematic). Each bin of the $q\eta_l$ distribution was fluctuated according to a Poission distribution with the expected number of events in that bin as the mean. The fluctuated $q\eta_l$ distribution was subject to the decomposition and extrapolation procedure to measure the $A_{\rm FB}^{\rm lep}$. The mean $A_{\rm FB}^{\rm lep}$ of 10k P.E is consistent with

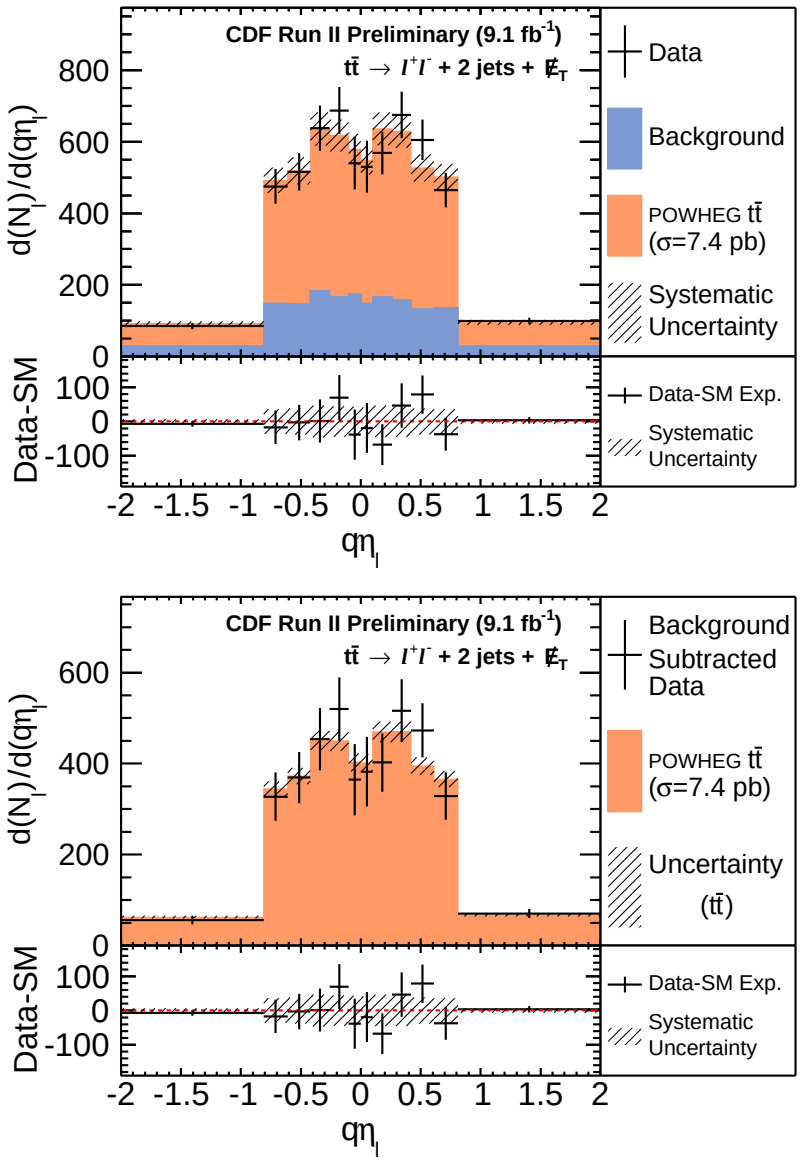

FIG. 10. A comparison of the observed $q\eta_l$ distribution along with the SM expectation. The figure on the bottom shows the same data, but after background subtraction.

the $A_{\rm FB}^{\rm lep}$ obtained before fluctuation, and the standard deviation, taken as the expected statistical uncertainty, is measured to be 0.043.

The uncertainty due to the background is estimated with a second set of pseudo-experiments in which both the $t\bar{t}$ signal and each background component are varied according to their mean rate and total rate uncertainties. Each bin of each component was fluctuated according to Poission distribution. Each pseudo-experiment was then analyzed using the same methodology as the data, but with the nominal background subtraction. The mean $A_{\rm FB}^{\rm lep}$ from the 10k P.E. was consistent with mean of previous P.E., and the σ (0.052) represents the statistical uncertainty from signal together with the uncertainty due to fluctuation in the backgrounds. The difference between two σ's in quadrature (0.029) is quoted as the background systematic uncertainty. As previously noted, this is the dominant systematic uncertainty in our measurement.

As explained in Sec. 3.3, we assign the difference between the measured $A_{\rm FB}^{\rm lep}$ and the $A_{\rm FB}^{\rm lep}$ at truth level from POWHEG $t\bar{t}$ MC as the asymmetric modelling systematic uncertainty to cover potential mismodelling introduced by the methodology for obtaining the parton level $A_{\rm FB}$. This has a value of 0.006. To estimate the systematic uncertainty due to the variation in the symmetric part of the $q\eta_l$ distribution from different physics model, which we call the

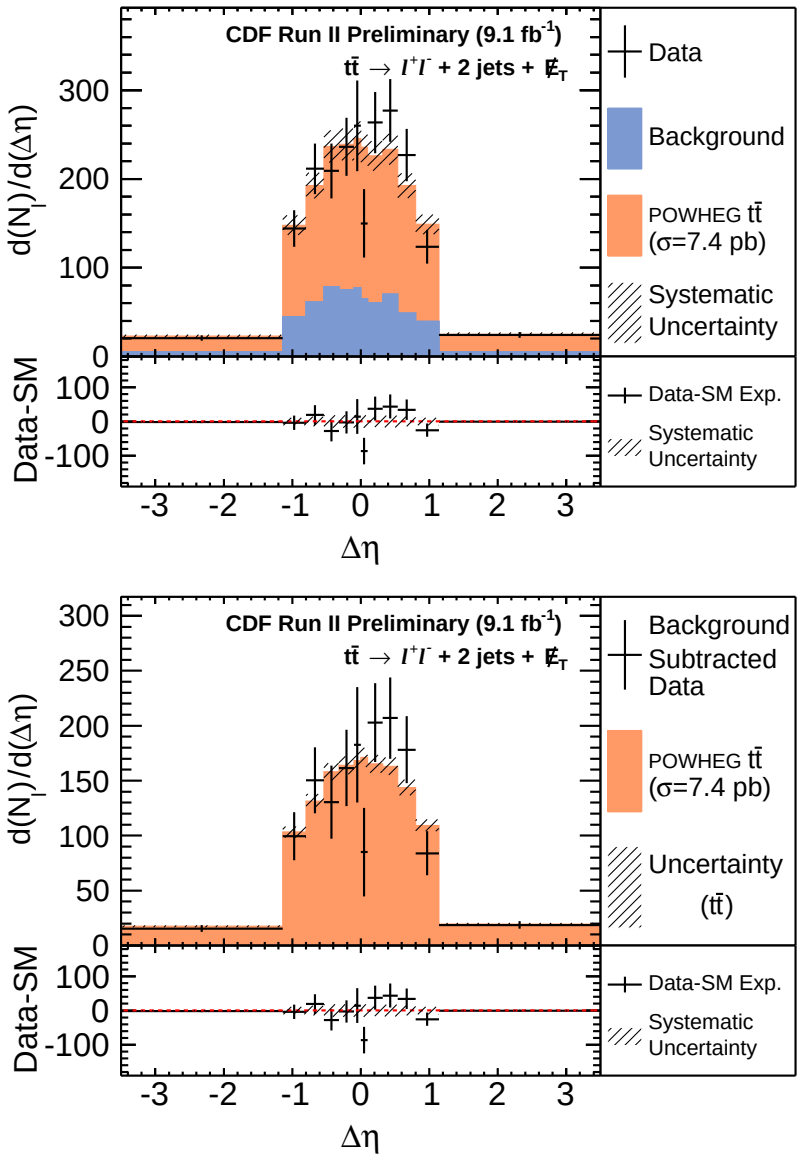

FIG. 11. A comparison of the observed $\Delta\eta$ distribution along with the SM expectation. The figure on the right shows the same data, but after background subtraction.

symmetric modelling uncertainty, we calculate $A_{\rm FB}^{\rm lep}$ with symmetric models from ALPGEN, PYTHIA, AxiL, AxiR and Axi0 $t\bar{t}$ samples, and take the largest difference between these $A_{\rm FB}^{\rm lep}$'s and the central value of measured $A_{\rm FB}^{\rm lep}$ with symmetric model from POWHEG $t\bar{t}$ MC. We find this to be 0.001, again small compared to the dominant uncertainty.

The Jet Energy Scale systematic uncertainty is estimated by simultaneously shifting the Jet Energy Scale up and down 1σ, and taking the larger difference between shifted $A_{\rm FB}^{\rm lep}$ and central value of measured $A_{\rm FB}^{\rm lep}$. This systematic uncertainty is estimated to be 0.004. We also estimated other systematics due to parton showering model, color reconnection, Initial/Final State Radiation, and Parton Distribution Function. They are found to be negligible, and thus not listed in Table VII, which summaries the systematic and statistical uncertainties. The total systematic uncertainty is 0.03, which is dominated by the systematic uncertainty of backgrounds.

After including all the systematic uncertainties, the $A_{\rm FB}^{\rm lep}$ is measured to be

$$A_{FB}^{lep} = 0.072 \pm 0.052(\text{stat.}) \pm 0.030(\text{sys.}) = 0.072 \pm 0.060$$

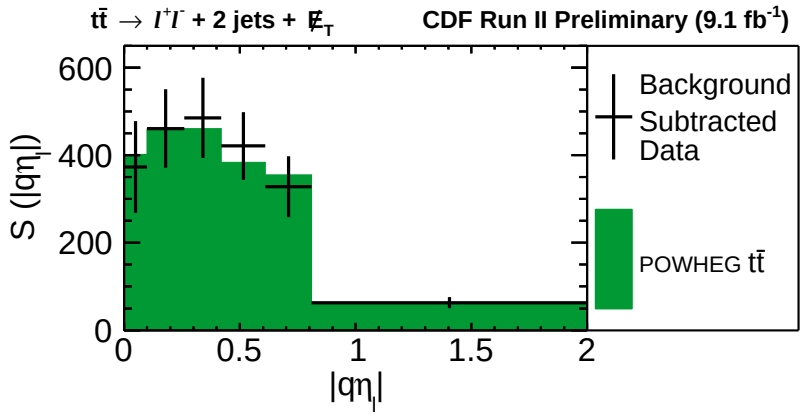

FIG. 12. Symmetric part of the $q\eta_l$ distribution from data after background subtraction with the expectations from POWHEG overlaid.

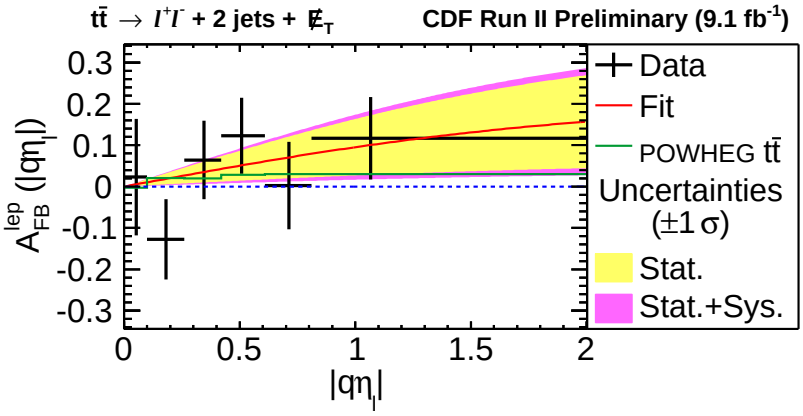

FIG. 13. Asymmetric part of $q\eta_l$ distribution from data after background subtraction. The green line shows the expectation from POWHEG MC.

4.3. Cross Checks

We performed the same measurement in several subsets of the data as cross checks. The subsets we used are with different lepton categories (ee, $\mu\mu$, and eμ), with different lepton charges (positive and negative leptons only), and with events with at least one Sec-Vtx b-tag [21] to increase the sample purity (although doing so lowers the overall

CDF Run II Preliminary (9.1 fb^{-1})	
Source of Uncertainty (A_{FB}^{lep})	Value
Backgrounds	0.029
Asymmetric Modeling	0.006
Jet Energy Scale	0.004
Symmetric Modeling	0.001
Total Systematic	0.030
Statistical	0.052
Total Uncertainty	0.060

TABLE VII. Table of uncertainties for the A_{FB}^{lep} measurement.

sensitivity due to smaller statistics). Also note that the luminosity for this data sample is smaller because it requires the silicon detector to be good for data taking. Table VIII shows results of the cross checks. The $A_{\rm FB}^{\rm lep}$ measured from all sub-categories are consistent with each other within statistics.

CDF Run II Preliminary (9.1 fb^{-1})

Category	$A_{\rm FB}^{\rm lep}$
All	0.072±0.052(stat)
ee	0.128±0.101(stat)
$\mu\mu$	0.075±0.117(stat)
eμ	0.044±0.070(stat)
Positive Lepton	0.099±0.073(stat)
Negative Lepton	0.043±0.070(stat)
w/ $\geq$ 1 b-tag*	0.105±0.063(stat)

* The integrated luminosity corresponding to events with b-tag is 8.7 fb^{-1}.

TABLE VIII. The measured values of $A_{\rm FB}^{\rm lep}$ in a number of different subsets of the data as a cross check for the result. The uncertainties are statistical only.

4.4. Measuring $A_{\rm FB}^{\Delta\eta}$

The same methods are applied to the $\Delta\eta$ distribution to extract $A_{\rm FB}^{\Delta\eta}$. The decomposition of the symmetric and asymmetric part of $\Delta\eta$ distribution are shown in Fig. 14 together with the fit. The uncertainties for $A_{\rm FB}^{\Delta\eta}$ measurement are estimated in the same way as measuring $A_{\rm FB}^{\rm lep}$, and are listed in Table IX. The final result for $A_{\rm FB}^{\Delta\eta}$ is:

$$A_{\rm FB}^{\Delta\eta} = 0.076 \pm 0.072(\text{stat.}) \pm 0.039(\text{sys.}) = 0.076 \pm 0.082$$

.

CDF Run II Preliminary (9.1 fb^{-1})

Source of Uncertainty ($A_{\rm FB}^{\Delta\eta}$)	Value
Backgrounds	0.037
Asymmetric Modeling	0.012
Jet Energy Scale	0.003
Symmetric Modeling	0.004
Total Systematic	0.039
Statistical	0.072
Total Uncertainty	0.082

TABLE IX. The table of uncertainties for $A_{\rm FB}^{\Delta\eta}$ measurement.

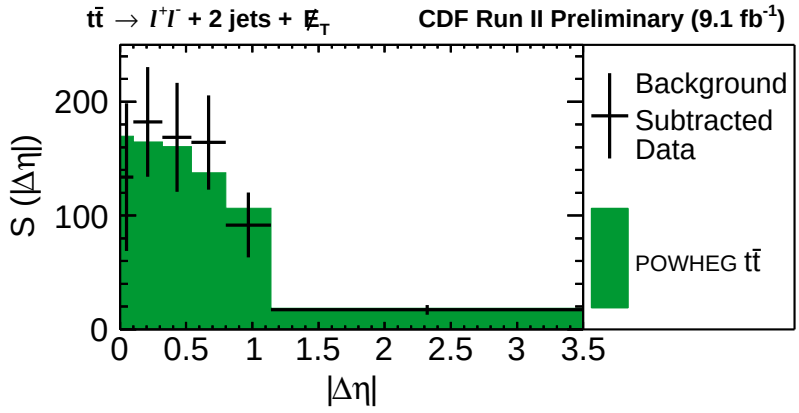

(a)

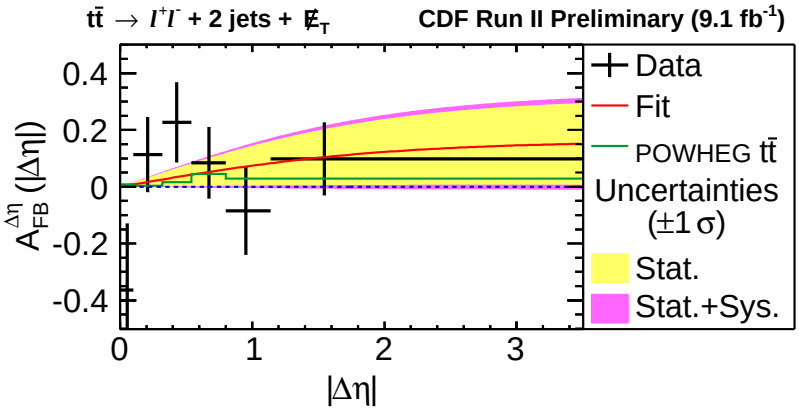

(b)

FIG. 14. The same figures as Fig. 12 and 13, but with $|\Delta\eta|$ instead of $|q\eta_l|$.

5. CDF COMBINATION OF CHARGE WEIGHTED LEPTONIC $A_{\rm FB}$

In this section we report the combination of the measurements of the charge weighted leptonic $A_{\rm FB}$ of $t\bar{t}$ system in the dilepton final state described in the previous sections and the same measurement in the lepton+jets final state in Ref. [13]. The combination is based on the Best Linear Unbiased Estimates (BLUE) [22] method. In order to deal with the asymmetric uncertainties in the measurement, we followed the approach of Asymmetric Iterative BLUE (AIB) [23].

The charge weighted leptonic $A_{\rm FB}$ measured in the lepton+jets final state [13] is:

$$A_{\rm FB}^{\rm lep} = 0.094 \pm 0.024({\rm stat.})^{+0.022}_{-0.017}({\rm sys.})$$

The two measurements are done in two orthogonal final states, thus the statistical uncertainties are uncorrelated. The two measurements share a small portion of the backgrounds, and the backgrounds systematic uncertainties are mainly caused by the uncertainties in the shape of the background $q\eta_l$ distributions, which are largely uncorrelated between the two measurements, thus the background uncertainties are treated as uncorrelated between the two measurements. The recoil modeling systematic uncertainty in the lepton+jets measurement and the asymmetric modeling systematic uncertainty in the dilepton measurement are both designed to cover the potential biases introduced by the methodology to correct for the detector response and the detector coverage, thus they are treated as fully correlated. The symmetric modeling systematic uncertainty is negligible in the measurement with the lepton+jets final state, thus only the corresponding uncertainty in the measurement with the dilepton final state is considered. The Jet Energy Scale systematic uncertainties in the two measurements are estimated in a fully correlated way, thus they are treated as fully correlated. The uncertainties due to color reconnection, parton showering, parton distribution functions and initial/final state radiation are negligible in the measurement with the dilepton final state, thus only the corresponding uncertainties with the lepton+jets final state are included. The uncertainties are summarized in Table X, as well as the correlations between the uncertainties in the two measurements.

CDF Run II Preliminary

Source of uncertainty	L+J (9.4fb^{-1})	DIL (9.1fb^{-1})	Correlation
Backgrounds	0.015	0.029	0
Recoil modeling (Asymmetric modeling)	$^{+0.013}_{-0.000}$	0.006	1
Symmetric modeling	-	0.001	
Color reconnection	0.0067	-	
Parton showering	0.0027	-	
PDF	0.0025	-	
JES	0.0022	0.004	1
IFSR	0.0018	-	
Total systematic	$^{+0.022}_{-0.017}$	0.030	
Statistics	0.024	0.052	0
Total uncertainty	$^{+0.032}_{-0.029}$	0.060	

TABLE X. Table of uncertainties for $A_{\rm FB}^{\rm lep}$ measurement in the lepton+jets and the dilepton final state. In the column of correlation, "0" indicates no correlation and "1" indicates fully positive correlation.

With the correlations between the uncertainties in the two measurements specified, we proceeded with the AIB procedure [23] to obtain the best measurement of the $A_{\rm FB}^{\rm lep}$ from CDF. The combined $A_{\rm FB}^{\rm lep}$ is

$$A_{\rm FB}^{\rm lep} = 0.090^{+0.028}_{-0.026}$$

The weight of the measurement with the lepton+jets final state in the combination is 80%, while the weight of the one with the dilepton final state is 20%. The correlation between the two measurements is estimated to be 2.6%.

6. CONCLUSION

We have measured the leptonic $A_{\rm FB}$ of $t\bar{t}$ with dilepton final state using data collected during CDF Run II. The results are:

$$A_{FB}^{lep} = 0.072 \pm 0.052({\rm stat.}) \pm 0.030({\rm sys.}) = 0.072 \pm 0.060$$

and

$$A_{\rm FB}^{\Delta\eta} = 0.076 \pm 0.072(\text{stat.}) \pm 0.039(\text{sys.}) = 0.076 \pm 0.082$$

The results are in consistent with prediction from NLO SM of $A_{\rm FB}^{\rm lep} = 0.038 \pm 0.003$ and $A_{\rm FB}^{\Delta\eta} = 0.048 \pm 0.004$ [1]. Furthermore we obtained the best measurement of the $A_{\rm FB}^{\rm lep}$ from CDF by combining the measurement in the lepton+jets final state with the measurement in the dilepton final state. The combined result is

$$A_{\rm FB}^{\rm lep} = 0.090^{+0.028}_{-0.026}$$

This result is 2σ larger than the NLO SM calculation at $A_{\rm FB}^{\rm lep} = 0.038 \pm 0.003$ [1]. The comparison of $A_{\rm FB}^{\rm lep}$ measurement from CDF is shown in Fig 15.

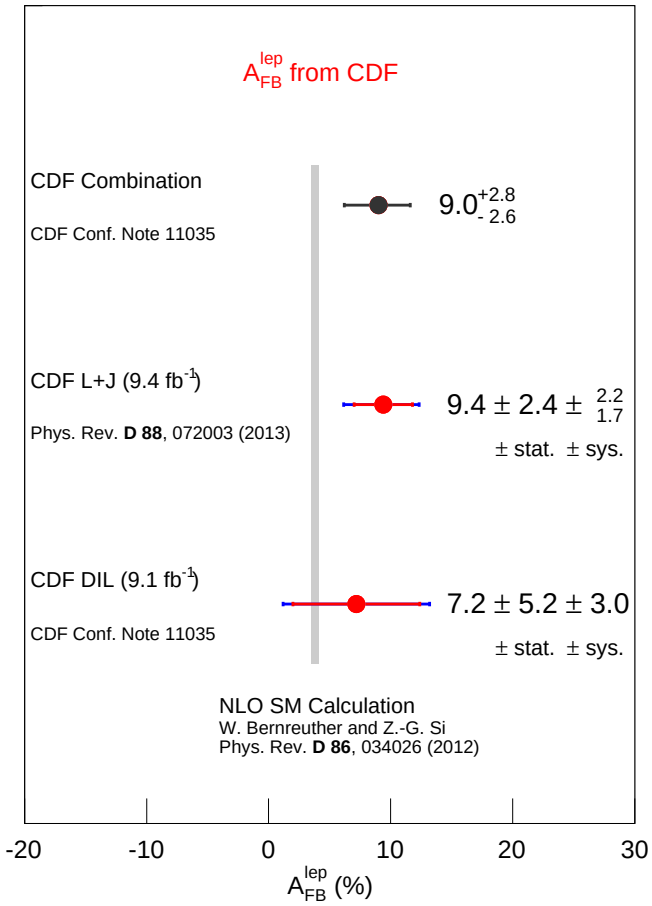

FIG. 15. Comparison of $A_{\rm FB}^{\rm lep}$ measurements with lepton+jets and dilepton final states from CDF.

ACKNOWLEDGMENTS

We thank the Fermilab staff and the technical staffs of the participating institutions for their vital contributions. This work was supported by the U.S. Department of Energy and National Science Foundation; the Italian Istituto Nazionale di Fisica Nucleare; the Ministry of Education, Culture, Sports, Science and Technology of Japan; the Natural Sciences and Engineering Research Council of Canada; the National Science Council of the Republic of China; the Swiss National Science Foundation; the A.P. Sloan Foundation; the Bundesministerium für Bildung und Forschung, Germany; the Korean World Class University Program, the National Research Foundation of Korea; the Science and Technology Facilities Council and the Royal Society, United Kingdom; the Russian Foundation for Basic

Research; the Ministerio de Ciencia e Innovación, and Programa Consolider-Ingenio 2010, Spain; the Slovak R&D Agency; the Academy of Finland; the Australian Research Council (ARC); and the EU community Marie Curie Fellowship Contract No. 302103.

[1] W. Bernreuther and Z.-G. Si, Phys. Rev. **D 86**, 034026 (2012).
[2] D.-W. Jung, P. Ko, and J. S. Lee, Phys. Lett. **B 701**, 248 (2011).
[3] D.-W. Jung, P. Ko, J. S. Lee, and S. hyeon Nam, Phys. Lett. **B 691**, 238 (2010); E. Álvarez, L. Rold, and A. Szynkman, J. of High Energy Phys. **2011**, 1 (2011); C.-H. Chen, G. Cvetic, and C. Kim, Phys. Lett. **B 694**, 393 (2011); Y.-k. Wang, B. Xiao, and S.-h. Zhu, Phys. Rev. **D 82**, 094011 (2010); A. Djouadi, G. Moreau, F. m. c. Richard, and R. K. Singh, *ibid.* **82**, 071702 (2010); R. S. Chivukula, E. H. Simmons, and C.-P. Yuan, *ibid.* **82**, 094009 (2010); B. Xiao, Y.-k. Wang, and S.-h. Zhu, *ibid.* **82**, 034026 (2010); Q.-H. Cao, D. McKeen, J. L. Rosner, G. Shaughnessy, and C. E. M. Wagner, *ibid.* **81**, 114004 (2010); I. Doršner, S. Fajfer, J. F. Kamenik, and N. Košnik, *ibid.* **81**, 055009 (2010); S. Jung, H. Murayama, A. Pierce, and J. D. Wells, *ibid.* **81**, 015004 (2010); J. Shu, T. M. P. Tait, and K. Wang, *ibid.* **81**, 034012 (2010); A. Arhrib, R. Benbrik, and C.-H. Chen, *ibid.* **82**, 034034 (2010); J. Cao, Z. Heng, L. Wu, and J. M. Yang, *ibid.* **81**, 014016 (2010); V. Barger, W.-Y. Keung, and C.-T. Yu, *ibid.* **81**, 113009 (2010); P. Ferrario and G. Rodrigo, *ibid.* **78**, 094018 (2008); **80**, 051701 (2009); M. Bauer, F. Goertz, U. Haisch, T. Pfoh, and S. Westhoff, J. of High Energy Phys. **2010**, 1 (2010); K. Cheung, W.-Y. Keung, and T.-C. Yuan, Phys. Lett. **B 682**, 287 (2009); P. H. Frampton, J. Shu, and K. Wang, **683**, 294 (2010).
[4] T. Aaltonen *et al.* (CDF Collaboration), Phys. Rev. **D 83**, 112003 (2011).
[5] V. Abazov *et al.* (D0 Collaboration), Phys. Rev. **D 84**, 112005 (2011).
[6] T. Aaltonen *et al.* (CDF Collaboration), CDF Public Note 10436 (2011).
[7] T. Aaltonen *et al.* (CDF Collaboration), (), arXiv:1306.2357 [hep-ex].
[8] A. Falkowski, M. L. Mangano, A. Martin, G. Perez, and J. Winter, Phys. Rev. **D 87**, 034039 (2013).
[9] T. Sjostrand, S. Mrenna, and P. Z. Skands, J. of High Energy Phys. **0605**, 026 (2006).
[10] M. L. Mangano, M. Moretti, F. Piccinini, R. Pittau, and A. D. Polosa, J. of High Energy Phys. **0307**, 001 (2003).
[11] S. Frixione, P. Nason, and G. Ridolfi, J. of High Energy Phys. **0709**, 126 (2007); P. Nason, **0411**, 040 (2004); S. Frixione, P. Nason, and C. Oleari, **0711**, 070 (2007); S. Alioli, P. Nason, C. Oleari, and E. Re, **1006**, 043 (2010).
[12] J. Alwall, P. Demin, S. de Visscher, R. Frederix, M. Herquet, *et al.*, J. of High Energy Phys. **0709**, 028 (2007).
[13] T. Aaltonen *et al.* (CDF Collaboration), Phys. Rev. **D 88**, 072003 (2013).
[14] V. Abazov *et al.* (D0 Collaboration), D0 Note 6394-CONF (2013).
[15] V. Abazov *et al.* (D0 Collaboration), arXiv:1308.6690 [hep-ex].
[16] T. Aaltonen *et al.* (CDF Collaboration), (), arXiv:1304.7961 [hep-ex].
[17] U. Baur, T. Han, and J. Ohnemus, Phys. Rev. **D 48**, 5140 (1993).
[18] E. Gerchtein and M. Paulini, eConf **C0303241**, TUMT005 (2003).
[19] S. Agostinelli *et al.*, Nucl. Instrum. Meth. A **506**, 250 (2003).
[20] M. Czakon and A. Mitov, arXiv:1112.5675 [hep-ph].
[21] D. Acosta *et al.* (CDF Collaboration), Phys. Rev. **D 71**, 052003 (2005).
[22] L. Lyons, D. Gibaut, and P. Clifford, Nucl. Instrum. Meth. A **270**, 110 (1988); L. Lyons, A. J. Martin, and D. H. Saxon, Phys. Rev. **D 41**, 982 (1990); A. Valassi, Nucl. Instrum. Meth. A **500**, 391 (2003).
[23] R. Group, C. Ciobanu, K. Lannon, and C. Plager (CDF Collaboration), in *Proceedings of the 34th International Conference in High Energy Physics (ICHEP08), Philadelphia, 2008, eConf C080730*, arXiv:0809.4670 [hep-ex].